Solvent Extraction and Ion Exchange

ISSN: 0736-6299 (Print) 1532-2262 (Online) Journal homepage: www.tandfonline.com/journals/lsei20

Nitric Acid and Water Extraction by T2EHDGA in *n*-Dodecane

Emily L Campbell, Vanessa E Holfeltz, Gabriel B Hall, Kenneth L Nash, Gregg J Lumetta & Tatiana G Levitskaia

To cite this article: Emily L Campbell, Vanessa E Holfeltz, Gabriel B Hall, Kenneth L Nash, Gregg J Lumetta & Tatiana G Levitskaia (2017) Nitric Acid and Water Extraction by T2EHDGA in *n*-Dodecane, Solvent Extraction and Ion Exchange, 35:7, 586-603, DOI: 10.1080/07366299.2017.1400161

To link to this article: https://doi.org/10.1080/07366299.2017.1400161

Published online: 06 Dec 2017.

SOLVENT EXTRACTION AND ION EXCHANGE
2017, VOL. 35, NO. 7, 586–603
https://doi.org/10.1080/07366299.2017.1400161

Taylor & Francis
Taylor & Francis Group

Nitric Acid and Water Extraction by T2EHDGA in *n*-Dodecane

Emily L Campbell[a,b], Vanessa E Holfeltz[a,c], Gabriel B Hall[a], Kenneth L Nash[b], Gregg J Lumetta [a], and Tatiana G Levitskaia[a]

[a]Pacific Northwest National Laboratory, Richland, Washington, USA; [b]Chemistry Department, Washington State University, Pullman, Washington, USA; [c]School of Nuclear Science and Engineering, Oregon State University, Corvallis, OR

ABSTRACT

Liquid–liquid distribution behavior of nitric acid (HNO_3) and water by a diglycolamide (DGA) ligand, *N,N,N′,N′*-tetra-2-ethylhexyldiglycolamide (T2EHDGA), into *n*-dodecane diluent was investigated. Spectroscopic Fourier transform infrared spectroscopy (FTIR) and nuclear magnetic resonance (NMR) characterization of the organic extraction solutions indicate the T2EHDGA carbonyl coordinates with HNO_3 and progressively aggregates at high acid conditions. Water extraction increases in the presence of HNO_3. The experimentally observed distribution of HNO_3 was modeled using the computer program SXLSQI. The results indicated that the formation of two organic-phase species —HNO_3·T2EHDGA and $(HNO_3)_2$·T2EHDGA—satisfactorily describes the acid distribution behavior. Temperature-dependent solvent extraction studies allowed for the determination of thermodynamic extraction constants and ΔH and ΔS parameters for the corresponding extractive processes.

KEYWORDS

ALSEP; T2EHDGA; speciation model; trivalent actinides and lanthanides; extraction constant

Introduction

Nuclear energy is a leading source of carbon-free electricity that is well established and capable of replacing a significant percentage of the base-load power generated by fossil fuels.[1] Current uranium resources needed to fuel nuclear reactors are predicted to last over 100 years, but increased energy demands and population growth are expected to significantly shorten the projected timeline if reprocessing is not considered.[2] In addition, the reprocessing of used nuclear fuel provides tangible benefits to the geological disposal of the by-products of nuclear power production, primarily in terms of increased repository capacity through reducing the heat loading, but also in terms of reducing the long-term radiotoxicity of the geologically disposed material.[3]

Minor actinides (MAs), such as americium (Am) and curium (Cm), are primary contributors to the thermal load and long-term radiotoxicity of intact spent nuclear fuel. Transmutation of these elements in a "Generation IV" (fast) reactor has been proposed as a method for high-level waste management in conjunction with a geological repository for short-lived fission products and lanthanides (Ln).[4–6] During transmutation, the Ln elements act as neutron poisons due to their high neutron-capture cross sections, significantly hindering the efficiency of actinide transmutation.[7] Thus, partitioning the MA from the Ln is necessary for efficient transmutation of the MA into shorter-lived fission products. However, this separation is a nontrivial challenge due to the similarity of the ionic radii of the MA and Ln, their most commonly found oxidation states, and consequently their chemical behavior.[8]

Developing new extractant molecules with high selectivity for Am and Cm has been a subject of investigation for decades.[9–11] Diamide-based extractants, capable of extracting tri-, tetra-, and hexavalent actinides from nuclear fuel, have gained considerable interest due to

CONTACT Tatiana G Levitskaia Tatiana.Levitskaia@pnnl.gov Pacific Northwest National Laboratory, PO Box 999 MSIN P7-25, Richland, WA 99352, USA

Color versions of one or more of the figures in the article can be found online at www.tandfonline.com/lsei.

more robust backward extraction (stripping) of MA compared with phosphorus-based extractants.[12–14] More recently, diglycolamides (DGAs), a class of diamide extractants containing an ether linkage between two amide groups, have been the focus of many separation groups working on actinide partitioning.[14] This class of extractants has noteworthy advantages for reprocessing applications. DGA extractants have proven to be better Ln and MA extractants than malonamides with a favorably high distribution ratio (*D*) for Am(III) in nitric acid (HNO_3) at moderate concentrations, as well as high solubility in processing-friendly organic solvents, high selectivity toward Am(III) over non-Ln fission products, and the added advantage of disposal via incineration.[9,13–15]

Of these DGA extractants, *N,N,N',N'*-tetraoctyldiglycolamide (TODGA) has been studied the most extensively and has proven successful in the development of the European separation processes, DIAMide EXtraction (DIAMEX) and Selective Actinide Extraction (SANEX).[9,15,16] The branched derivative, *N,N,N',N'*-tetra-2-ethylhexyldiglycolamide (T2EHDGA), exhibits poorer extraction efficiency toward Am(III) compared with TODGA, presumably due to the greater steric congestion around the amide functionality. However, the weaker extractability of T2EHDGA toward light Ln has proven useful in the development of the Actinide Lanthanide SEParation (ALSEP) concept, specifically, to direct lanthanum to the raffinate during the first extraction step, which significantly decreases the metal loading in the organic phase from the extraction of subsequent Ln.[17,18]

The ALSEP concept uses an organic solvent that combines the neutral DGA extractant, T2EHDGA, and the acidic extractant 2-ethylhexylphosphonic acid mono-(2-ethylhexyl) ester (HEH[EHP]) to selectively co-extract Ln and MA from an acidic (3–4 M HNO_3) post- Plutonium Uranium Redox EXtraction (PUREX) raffinate. The MAs are then stripped back into the aqueous phase using a buffered polyaminocarboxylic acid solution, while the trivalent Ln remain in the organic phase, complexed by HEH[EHP].

DGA extractants have shown significant extraction capacity for HNO_3 into the nonpolar organic phase, along with a hyper-stoichiometric nitrate dependence on the extraction of trivalent *f*-elements from the HNO_3 media.[5,12] As amidic extractants, DGAs act as Lewis bases and have the potential to form adducts with HNO_3. The formation of such adducts decreases the concentration of free extractant available to participate in metal extraction and thus theoretically decreases the *D* values of trivalent Ln and MA. However, the opposite has been reported with the non-branched DGA, TODGA, where the *D* values of Am(III) are significantly enhanced in HNO_3 media compared with $NaNO_3$.[19] This suggests HNO_3 is participating in and/or facilitating the formation of the extracted Am(III) complex. Therefore, it is crucial to fundamentally understand the HNO_3 extraction behavior in these systems before prediction of the organic-phase speciation of Ln and MA is possible.[5] The present work is focused on characterizing the effects of HNO_3 and water extraction on the solvent modifications of T2EHDGA in *n*-dodecane.

Experimental

Materials

T2EHDGA was purchased from Eichrom Technologies and purified by column chromatography using a gradient elution of 100% dichloromethane to 100% diethyl ether. The identity of the purified product was consistent with that expected for T2EHDGA through characterization by ^{1}H NMR (nuclear magnetic resonance) and ^{13}C NMR spectroscopies, Fourier transform infrared spectroscopy (FTIR), UV-Vis spectrophotometry, and Electrospray Ionization mass spectrometry (ESI-MS).

All aqueous solutions were prepared using distilled water deionized to >18.2 MΩ (DIW). TraceSELECT 16 M HNO_3 (Fluka) was used for the preparation of aqueous HNO_3 solutions and standardized using Titrando Metrohm 905 Automatic Titrator against NaOH. Normal dodecane 99+ % was obtained from Alfa Aesar and used as received. Reagents not specifically mentioned were of analytical grade and used as received.

Solvent extraction experiments

A kinetic experiment was performed to determine the contact time required to reach equilibrium for HNO_3 extraction. Equal volumes of 0.1 M T2EHDGA/*n*-dodecane and 1.5 M HNO_3 were contacted at 25°C for the following equilibration times: 1, 5, 10, 15, 30, 45, 60, and 90 min and 2, 4, and 6 h. The organic phase was stripped by contact with deionized water and dilutions were performed as outlined below. The results indicated that equilibrium was achieved after 5 min of contact time.

To determine the HNO_3 extraction mechanism, samples of 0.1 M T2EHDGA in *n*-dodecane were contacted with equal volumes of 0.1–3 M HNO_3, in duplicate, on a shaker table at 300 rpm for 1 h with temperatures ranging from 25 to 50°C. The high-end 3 M HNO_3 concentration constraint was applied to avoid formation of the third phase observed in this system at greater HNO_3 concentrations. Temperature was maintained at ±1°C using a temperature-controlled box to house the shaker table. The samples were centrifuged for 2 min after mixing, and then separated into different vials where an aliquot of the organic phase was removed for stripping with DI water three successive times at an organic-to-aqueous phase volume ratio O/A = 0.5; the three aqueous stripping solutions were then combined to analyze the acid concentration of the combined solution.

Dependence of the HNO_3 extraction on the organic ligand concentration was studied at 25°C. The extractant concentration was varied from 0.01 to 0.2 M T2EHDGA in *n*-dodecane with an aqueous phase acid concentration fixed at 2.08 M HNO_3.

Duplicate experiments were performed for every data point. For proper weighting of the data in SXLSQI modeling (see below), experimental precision for each data point was assumed to be ±7% as estimated from a combination of replicate determinations, volumetric error, and the precision of analytical HNO_3 determinations by ion chromatography (IC) as described next. The minimum detectable extraction of HNO_3 corresponds to a D of 1×10^{-3}. In the control experiment, HNO_3 extraction into *n*-dodecane in the absence of T2EHDGA was tested, and the organic HNO_3 concentration was found to be below the minimum detectable limit, confirming that there was no significant extraction of HNO_3 into the neat diluent.

IC for NO_3^- determination

Stock HNO_3 solutions, post-contacted aqueous phase, and the aqueous samples generated by stripping of the organic phase were diluted using Grade A volumetric flasks, filtered through a 0.45 μm syringe filter, and analyzed with a Dionex ICS 5000 ion chromatograph. The ICS 5000 was equipped with a 2-mm-diameter AS-18 column, and the samples were analyzed at a flow rate of 0.35 mL/min. The IC system was equipped with reagent-free components where KOH eluent generation is automated and the suppression is self-regenerating. The recovery of HNO_3 based on mass balance was observed to be 99 ± 0.7% for all samples.

Extraction data treatment

Thermodynamic analysis of the equilibrium HNO_3 distribution data expressed in terms of D_{HNO3}, defined as:

$$D_{HNO_3} = \frac{[HNO_3]_{organic}}{[HNO_3]_{aqueous}} \tag{1}$$

was facilitated by the solvent extraction modeling program SXLSQI.[20] SXLSQI utilizes a combination of Pitzer parameters and Debye–Hückel treatment to account for the variation of activity coefficients of solute species and water activity in the aqueous phase, and the Hildebrand–Scott treatment to account for activity effects of the solute species in the organic phase.[21,22] The program converts the molar concentration to the molality scale in the Pitzer treatment using Masson coefficients and all constants are corrected to infinite dilution.[23] The solubility parameters and

Table 1. Parameters used in SXLSQI modeling.[20]

Ion		V_0 (cm^3 mol^{-1})		Sv^* (cm^3 $L^{1/2}$ $mol^{-3/2}$)	
Masson coefficients[a]					
NO_3^-		29.33		0.543	
Interaction	Temperature (°C)	$\beta^{(0)}$	$\beta^{(1)}$	$C\phi$	α
Pitzer parameters[25,26][b]					
H^+–NO_3^-	25	0.1168	0.3546	–0.00539	2.0
	35	0.1096	0.4383	0.00351	2.0
	40	0.1106	0.4453	0.00376	2.0
	50	0.1111	0.4610	0.00476	2.0
Species		V_0^c (cm^3 mol^{-1})		δ^d ($J^{1/2}$ $cm^{-3/2}$)	
Other parameters					
n-dodecane		228.6[e]		16.1[e]	
T2EHDGA		606.6[f]		19.15[f]	
T2EHDGA·HNO_3		-		22.6 ± 0.5[g]	
$(HNO_3)_2$·T2EHDGA		-		21.9 ± 1.9[g]	

[a] Masson coefficients taken from ref 23.
[b] Pitzer parameters corresponding to 25°C taken from ref 26. Pitzer parameters corresponding to 35–50°C calculated as described in ref 27.
[c] Molar volumes of the species in the organic phase.
[d] Hildebrand solubility parameters.
[e] Values taken from ref 24.
[f] Values estimated according to group contributions as described in ref 24.
[g] The solubility parameter of the complex was refined in this work.

molar volumes of the DGA ligand were estimated from group contributions and the solubility parameters of the organic product species were refined by the program.[24] Modeling parameter inputs for SXLSQI are summarized in Table 1. Comparison of the calculated *D* values to the experimental distribution data using the refined extraction constants indicates an agreement factor that reflects the goodness as fit.[25]

HNO_3 distribution results from data sets with variable T2EHDGA concentrations and variable aqueous HNO_3 at 25°C were used as input to the solvent extraction modeling program. Pitzer parameters for HNO_3 at 25°C were supplied in order to calculate the non-ideality effects in the aqueous phase.[25] The solubility parameter of T2EHDGA was calculated using group contributions as outlined elsewhere to account for activity effects in the organic phase.[24]

An extraction model consisting of two organic-phase species, HNO_3·T2EHDGA and $(HNO_3)_2$·T2EHDGA, was assumed based on the results of the NMR, FTIR, and vapor pressure osmometry (VPO) aggregation measurements (see below); the refinement of the corresponding extraction constants was determined via SXLSQI based on input of the combined experimental data sets. This two-species model was then used to predict the extraction constants for the temperature-dependent extraction data sets with D_{HNO3} from variable HNO_3 concentrations. Temperature adjustment to Pitzer parameters as described elsewhere was necessary for refinement of the extraction constants for variable-temperature experiments.[26]

Karl Fischer titration for H_2O partitioning

The partitioning of water into T2EHDGA solutions in *n*-dodecane was analyzed under conditions of variable extractant and variable HNO_3 concentrations. Equal volumes of organic solutions and water and/or HNO_3 were contacted on a shaker table at 300 rpm for 1 h at a temperature of 25°C. Sample aliquots were analyzed by Aquatest 2010 Karl-Fischer Coulometric Moisture Titrator in at least duplicate measurements. The experimental error was estimated at ±6% unless otherwise noticed. Experimentally determined water partitioning to *n*-dodecane was accounted for during the analysis.

Vapor pressure osmometry

Aggregation of T2EHDGA in *n*-heptane at room temperature (23 ± 1°C) was evaluated using a Vapro Wescor 5520 instrument. Bibenzyl in *n*-heptane was used as a monomeric calibration standard, which gave an instrument response of 7750 ± 290 mmol/kg over the entirety of experiments conducted. Bibenzyl was procured from Aldrich at 99% purity and recrystallized twice from methanol prior to use.

The molality of the organic solutions was varied from 0 to 0.3 molal for bibenzyl and T2EHDGA. T2EHDGA solutions were contacted with 0–5 M HNO_3 for 1 h at 25°C and measured in at least triplicate, with a typical precision of ±3%.

Fourier transform infrared spectroscopy

FTIR measurements were conducted using a Bruker ALPHA Platinum ATR module with a single reflection diamond cell at room temperature (23 ± 1°C). Organic liquids were measured by placing a drop of the tested solution directly on the diamond plate. Each measurement consisted of 24 scans averaged with a resolution of 4 cm^{-1}. Background measurements of air were taken between each sample after cleaning with an appropriate solvent.

NMR spectroscopy

Hetero nuclear (^{13}C, ^{1}H, and ^{15}N) NMR spectroscopy was used to investigate the structural effects of HNO_3 extraction on 0.1 M T2EHDGA in *n*-dodecane at 25°C. ^{1}H, ^{13}C, and ^{15}N NMR measurements were run with a 500 MHz Oxford magnet and an Agilent DD2 console using a 5 mm, OneNMR probe. The ^{13}C and ^{15}N spectra were obtained using a 1-d gated decoupling pulse sequence. Additional parameters for the ^{15}N experiment were 15 µs for the rf 90 pulse, 10 s recycle delay, 1 s acquisition time, with a total of at least 42,000 scans collected per sample. Acetone-d6, 99.9 atom % D (Cambridge Isotope Labs), was used in a coaxial insert for ^{13}C NMR as an internal reference with the acetone carbonyl referenced to 206.26 ppm. The ^{15}N NMR spectra were externally referenced to 90% formamide at –267.8 ppm.[28,29]

Results and discussion

Extraction of water by T2EHDGA

Results of the water extraction process by T2EHDGA over concentrations in the range 0.01–0.20 M in *n*-dodecane as obtained by Karl Fischer analysis are shown in Figure 1A. Organic-phase water concentrations gradually increased along with the T2EHDGA concentration. Moderate water extraction is observed for the entire T2EHDGA concentration range, resulting in an approximately 0.15 molar ratio of H_2O to T2EHDGA in the organic phase; for example, $[H_2O]_{org}$ was 30 mM at 0.20 M T2EHDGA. An enhancement in the amount of water extracted occurs when *n*-dodecane solutions containing variable concentrations of T2EHDGA are contacted with 2 M HNO_3 compared with the contact with pure water (Figure 1A), and the concentration of water in the organic phase increases from 30 mM at 0.2 M T2EHDGA to greater than 80 mM.

The results obtained from a study of the extraction of water into 0.1 M T2EHDGA in *n*-dodecane from variable HNO_3 contacts are summarized in Figure 1B. The water content of 0.10 M T2EHDGA in *n*-dodecane in equilibrium with pure water was 0.017 ($\pm 1.5 \times 10^{-3}$) M. Upon contact with low concentrations of HNO_3 (0.1–0.5 M), the concentration of water in the organic phase does not differ from water extraction by 0.1 M T2EHDGA until the equilibrium aqueous acidity reaches 1 M HNO_3, at which point a sharp increase in water extraction is observed. The organic-phase water concentration from 0.1 M T2EHDGA in equilibrium with pure water was subtracted from the water content measured in the organic phase post-contact with variable concentrations of HNO_3 (0.1–3 M) and

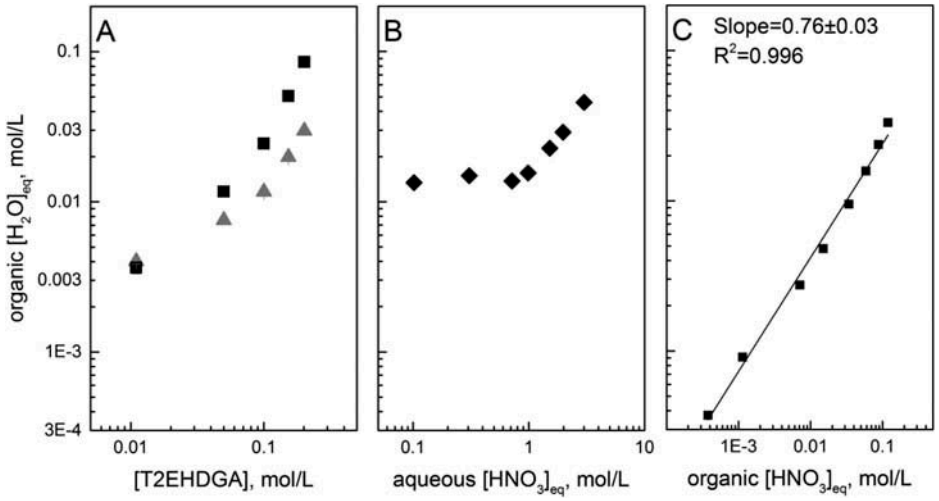

Figure 1. Water concentration in the equilibrium T2EHDGA / *n*-dodecane extraction solutions as a function of T2EHDGA concentration in *n*-dodecane solutions contacted with (▲) H2O and (■) 2 M HNO_3 (A) and HNO_3 concentration in aqueous (B) or organic (C) solutions obtained by equilibration of the 0.1 M T2EHDGA/n-dodecane with variable aqueous HNO_3 solutions. Panes (A) and (B) show total organic water concentration corrected for the water extracted by *n*-dodecane diluent at 25 °C. Pane (C) shows organic water concentration co-extracted with nitric acid and determined by the difference of the water concentrations corresponding to the HNO_3-saturated and water-saturated 0.1 M T2EHDGA/n-dodecane solutions.

plotted against organic HNO_3 concentration to determine water co-extracted with HNO_3 (Figure 1C). The observed linear dependence with a slope approaching 1 indicates that the concentration ratio of extracted HNO_3 to co-extracted water remains constant at $[HNO_3]/[H_2O] = 3.6 \pm 0.2$ once aqueous acidity exceeds 1 M HNO_3.

Interestingly, FTIR and Raman analysis of the T2EHDGA/*n*-dodecane solutions equilibrated with water and/or HNO_3 do not show the characteristic O–H vibrational envelopes at 2500–2600 or 3100–3700 cm^{-1}. This suggests that the symmetry of the water in the organic phase is significantly altered in such a way that the vibrational modes become spectroscopically silent; further studies are warranted to explain this result.

Aggregation of T2EHDGA *in* n-*dodecane by VPO*

VPO is a useful tool for determining aggregation behavior in organic solutions. By comparing the instrument responses for solutions containing variable ligand concentrations against a monomeric standard, the average aggregation number can be deduced from the ratio of the slopes.

In this experiment, *n*-heptane was substituted for *n*-dodecane as the organic diluent to attain sufficient volatility of the solvent for adequate instrument response. The instrument response of T2EHDGA (from concentrations of 0–0.2 M, which corresponds to 0–0.3 molal in *n*-heptane) was measured both in the pristine solvent and after contact with aqueous 0–5 M HNO_3 solutions. The VPO response for the entire T2EHDGA concentration range was observed to be linear for both the pristine solvent and the solvent contacted with 0–2 M HNO_3 aqueous solutions. More complicated behavior was observed in the extraction systems with aqueous HNO_3 exceeding 2 M as described below.

The average T2EHDGA aggregation in the pristine solutions is 1.26 ± 0.03, suggesting a mixture of monomeric and higher-order dimeric species (Table 2). However, upon water washing of the organic solvent, the average aggregation number drops to 0.99 ± 0.06, indicating monomeric T2EHDGA species. These results are attributed to water facilitating the dissociation of dimers that form through van der Waals forces, likely interacting via carbonyl groups, and replacing one T2EHDGA in the dimer with hydrogen-bonded water. This is presumably why a lack of change of the carbonyl resonance upon equilibrating the organic solvent with water is observed by the ^{13}C NMR studies.

Table 2. Average aggregation number of T2EHDGA in *n*-heptane as determined by VPO at room temperature (23 ± 1°C). Values corresponding to 2–5 M HNO_3 extraction systems were obtained using the VPO instrument response shown in Figure 2.

Contact conditions	Average aggregation number
Pristine	1.26 ± 0.03
H_2O saturated	0.99 ± 0.06
0.3 M HNO_3	1.13 ± 0.02
1 M HNO_3	1.15 ± 0.02
2 M HNO_3	0.98 ± 0.03
3 M HNO_3	1.08 ± 0.06
Above 0.14 m	1.93 ± 0.23
4 M HNO_3	1.47 ± 0.07
Above 0.14 m	2.42 ± 1.2
5 M HNO_3	1.7 ± 0.2
Above 0.14 m	4.6 ± 1.3

The presence of HNO_3 in the extraction systems at 2 M or below did not significantly change the average aggregation number of T2EHDGA, which remained close to unity for the entire T2EHDGA concentration range (Table 2). However, for the 3, 4, and 5 M HNO_3 systems, the VPO response exhibited two distinct regions (Figure 2). The first region, corresponding to the 0.01–0.14 molal (0.005–0.1 M) concentration range of T2EHDGA, is linear in all three systems; however, the slope gradually increases from 1.08 ± 0.06 at 3 M HNO_3 to 1.5 ± 0.07 and 1.7 ± 0.2 at 4 and 5 M HNO_3, respectively. This indicates that HNO_3 extraction from 4 M and more concentrated aqueous solutions causes the progressive formation of higher-order aggregates, even in dilute T2EHDGA solutions. In 3, 4, and 5 M HNO_3 systems, there is strong evidence of further T2EHDGA aggregation, as provided by the appearance of a second approximately linear region at and above 0.14 molal (0.1 M) T2EHDGA (Figure 2), with the respective average aggregation numbers 1.9 ± 0.2, 2.4 ± 1.2, and 4.6 ± 1.3 (Table 2). The deviation from linearity with increasing HNO_3 concentration is a qualitative observation

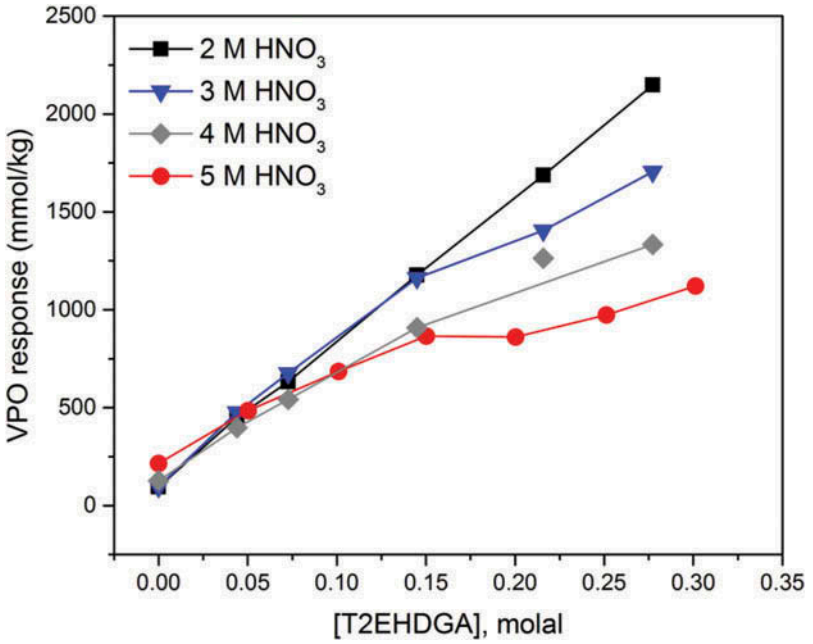

Figure 2. VPO instrument response for variable 0.05–0.3 molal (0.03–0.20 M) concentration T2EHDGA solutions in *n*-heptane contacted with variable concentrations of HNO_3 at room temperature (23 ± 1°C).

of extensive aggregation in those regimes. These results support a conclusion that there is both an aqueous acidity threshold and a critical ligand concentration, estimated at around 0.1 M, that must be reached for the extensive aggregation phenomenon to be observed. These findings are consistent with the observations of water uptake with TODGA by Yaita et al. and Jensen et al., where reverse-micelle tetramers were used to explain the high water and acid uptake, and a critical micelle concentration (CMC) of 0.7 M HNO_3 for 0.1 M TODGA/*n*-dodecane was reported.[12,30]

The abrupt change in the T2EHDGA/*n*-heptane osmolality plots, due the appearance of new extensive aggregation regimes upon equilibration with aqueous solutions containing HNO_3 at concentrations of 3 M and greater, is consistent with the HNO_3 distribution studies in T2EHDGA with *n*-dodecane. It was observed that organic HNO_3 concentration in the 0.1 M T2EHDGA/*n*-dodecane solution equilibrated with 3 M HNO_3 is 0.12 M, which exceeds 100% extractant loading considering only a 1:1 HNO_3·T2EHDGA complex, and therefore the formation of the high-order aggregates with greater than 1:1 stoichiometry is anticipated. In fact, visible third-phase formation was found to be prevalent with high HNO_3 concentrations and was optically observed for 0.14 molal (0.1 M) T2EHDGA at concentrations above 5 M HNO_3. This result is consistent with the study by Deepika et al., who observed the formation of the third phase for 0.2 M T2EHDGA/*n*-dodecane above 3.9 M HNO_3.[31] Similarly, 0.1 M TODGA/*n*-dodecane system has been reported to form a third phase upon equilibration with aqueous solutions containing HNO_3 at 3 M and above.[32–34] Although both extractant molecules possess three polar oxygen atoms, it has been suggested that third-phase formation with the branched DGA occurs prior to conditions necessary for the third-phase formation of TODGA.[35]

In summary, quantitative analytical results of super-stoichiometric quantities of water and HNO_3 in conjunction with aggregation measurements by VPO strongly suggest the presence of polar-core aggregates that are capable of solubilizing large quantities of polar solutes in nonpolar alkane diluents.[12,30]

HNO_3 distribution studies

Based on our VPO experiments and literature observations described above, to avoid third-phase formation, the investigation of HNO_3 distribution behavior was limited to aqueous concentrations below 3 M HNO_3.[31] In addition, HNO_3 recovery was determined for each sample to ensure that the extraction systems contained no third phase.

The *D* values for the extraction of HNO_3 from variable HNO_3 concentrations by T2EHDGA in *n*-dodecane at 25°C are presented in Figure 3A as a function of the initial HNO_3 concentration. These data were combined with the HNO_3 distribution data obtained as a function of the T2EHDGA concentration at 25°C (Figure 3B), and both data sets were supplied to the SXLSQI program. The model with two organic species consisted of 1:1 and 2:1 HNO_3:T2EHDGA complex species assumed based on the VPO, FTIR, and NMR results (described elsewhere in this manuscript), which was used to fit the extraction data. The best SXLSQI fit to the HNO_3 extraction data shown in Figure 3 by the solid lines was obtained using the following equilibrium reactions:

$$H^+ + NO_3^- + \overline{T2EHDGA}\ \overline{HNO_3} \rightleftharpoons \overline{T2EHDGA}\ K_{ex1} \tag{2}$$

$$2H^+ + 2NO_3^- + \overline{T2EHDGA}\overline{(HNO_3)_2} \rightleftharpoons \overline{T2EHDGA}\ K_{ex2} \tag{3}$$

Table 3 presents the refined equilibrium constants for Equations 2 and 3 using the non-ideality parameters listed in Table 1. There is satisfactory agreement between the experimental and calculated values obtained with the simple model represented by Equations 2 and 3 up to 2 M HNO_3 in the aqueous phase and 0.2 M T2EHDGA in the organic phase. The calculated *D* value for 3 M HNO_3 underestimates the corresponding experimental value, presumably due to the formation of larger aggregates in this concentration regime as indicated by VPO measurements but not accounted for by the supplied model.

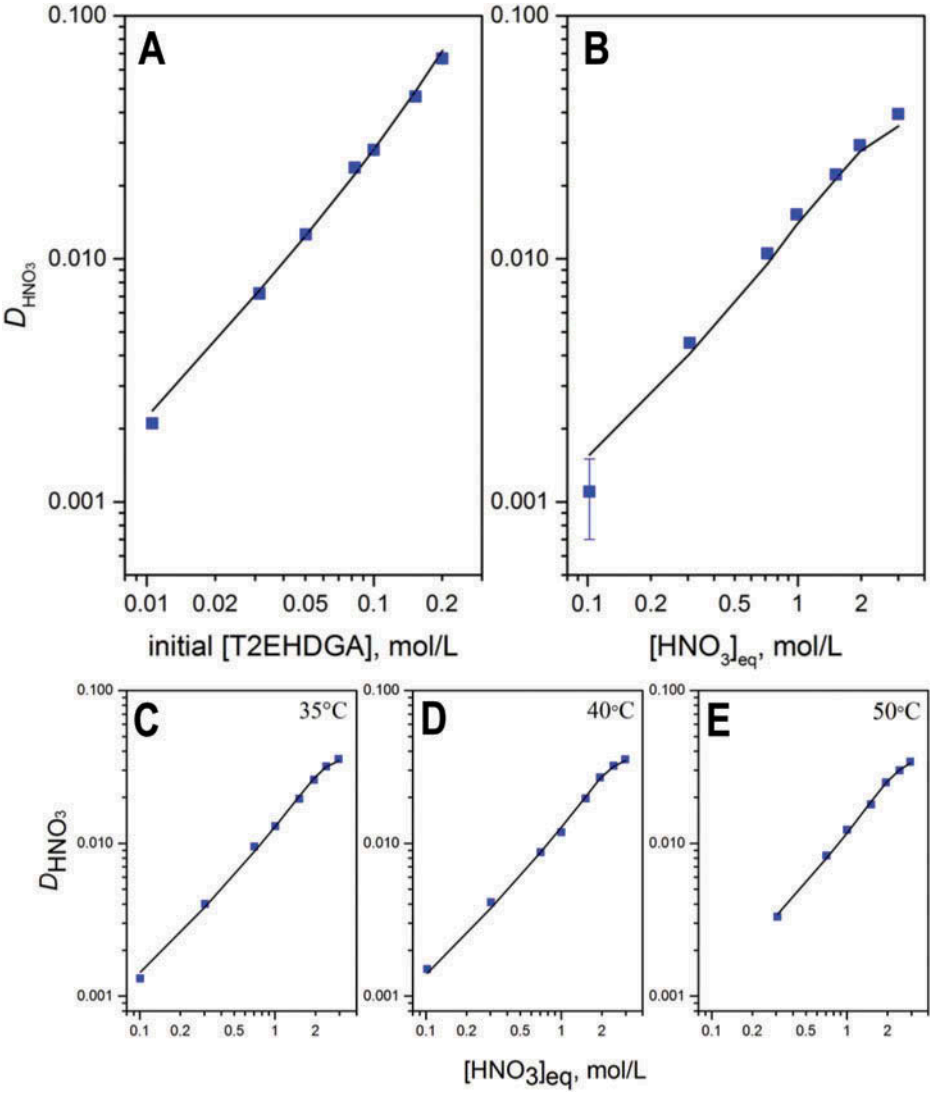

Figure 3. Dependence of the HNO_3 extraction distribution ratio on T2EHDGA concentration in *n*-dodecane at constant aqueous 2.0 M HNO_3 at 25°C (A) and equilibrium concentration of HNO_3 at constant 0.1 M T2EHDGA in *n*-dodecane at 25°C (B), 35°C (C), 40°C (D), and 50°C (E). All data points were obtained at least in duplicate. The solid lines are calculated values based on the model described in the text.

Table 3. Equilibrium constants corresponding to Equations 2 and 3 for the extraction of HNO_3 by T2EHDGA at 25–50°C as refined by SXLSQI.

Temperature (°C)	Log K_{ex1}	Log K_{ex2}	σ[a]
25	−0.76 ± 0.03	−2.0 ± 0.1	1.85
35	−0.81 ± 0.01	−2.29 ± 0.07	0.94
40	−0.82 ± 0.01	−2.31 ± 0.08	1.02
50	−0.87 ± 0.01	−2.46 ± 0.06	0.75

[a] Agreement factor quantifying the goodness of fit for a particular model to the given data set and defined according to the least-squares criterion as $\sigma = [\Sigma wi(Yi - Yc,i)^2/(No - Np)]^{1/2}$, where *Yi* is the *i*th experimentally observed quantity (i.e., *D*), *Yc,i* is the corresponding quantity calculated from the model being tested, *wi* is the weighting factor, defined as the reciprocal of the square of the estimated uncertainty of *Yi*, *No* is the number of observations, and *Np* is the number of adjustable parameters (i.e., log *K* values). The value of σ approaches one when the error of fitting is equal to the estimated experimental error; values less than one are interpreted as experimental precision greater than precision predicted with fitting.[21]

Conditional HNO_3 extraction constants have been reported in the literature for a variety of different DGA ligands. The log K value reported for single HNO_3·T2EHDGA species in n-dodecane at 1 M HNO_3 and obtained at 25°C varies from −0.72, as reported by Deepika et al., to 0.25, as reported by Gujar et al.[31,36] TODGA is assumed to form a 1:1 HNO_3·TODGA complex with log K values reported by Arisaka et al. and Gujar et al. of −0.42 and 0.61, respectively, from 1 M HNO_3 and n-dodecane as the diluent.[36,37] All these models utilize the HNO_3·DGA complex and account for free ligand by assuming all HNO_3 in the organic phase exists as the 1:1 complex. The results of our study indicate that more than just the 1:1 species is responsible for the extraction of HNO_3 with log K values of −0.76 ± 0.03 and −2.0 ± 0.1 for HNO_3·T2EHDGA and $(HNO_3)_2$·T2EHDGA, respectively. The calculated log K_{ex1} value for the 1:1 species in this experiment agrees well with the log K_{ex} value reported by Deepika et al. for T2EHDGA. However, without the inclusion of the higher-order HNO_3 species in the model, the predicted D of HNO_3 at moderate concentrations (1–3) M plateaus, contrary to experimental observations. This is indicative of saturation of the organic phase with HNO_3 due to complete ligand loading of the 1:1 species.

HNO_3 extraction as a function of temperature was investigated for 0.1 M T2EHDGA in n-dodecane with variable aqueous HNO_3 solutions from 25 to 50°C, as shown in Figure 3 (C–E). The results indicate a slight decrease in the distribution of HNO_3 as the temperature increases, suggesting exothermic behavior. These data sets were supplied to SXLSQI to determine the equilibrium extraction constants for Equations 2 and 3 at variable temperatures as reported in Table 3. Temperature-adjusted Pitzer parameters were calculated from a method described elsewhere, and the solubility parameters refined at 25°C were used for the variable-temperature data sets.[26] Excellent agreement between the experimental and calculated D values was observed.

A Van't Hoff plot was constructed to determine the thermodynamic parameters, ΔH and ΔS, for reactions 1 and 2 from the thermodynamic extraction constant calculated by SXLSQI through the following relationship:

$$lnK_{ex} = -\frac{\Delta H}{RT} + \frac{\Delta S}{R} \tag{4}$$

where R is the molar gas constant and T is the temperature in Kelvin. The Van't Hoff plot in Figure 4 indicates that the formation of $(HNO_3)_2$·T2EHDGA species is more temperature-dependent than the 1:1 species. The positive slopes of 0.96 ± 0.07 and 3.4 ± 0.5 attained from the Van't Hoff plot indicate that the extractions of both product species in the organic phase are exothermic reactions and confirmed by the negative enthalpy values in Figure 4. The relatively flat slopes suggest that the extraction of HNO_3 is not strongly temperature-dependent at the range 25–50°C. The extraction of both species is driven by an exothermic enthalpy term compensating an unfavorable entropy term. The negative ΔS for the extraction of HNO_3 implies that the extracted HNO_3 promotes ordering of the system. Presumably, the greater magnitude of ΔS for the higher-order $(HNO_3)_2$·T2EHDGA species compared with HNO_3·T2EHDGA can be explained by the greater number of reactant species necessary to form $(HNO_3)_2$·T2EHDGA and consequently the greater number of intermolecular interactions involved.

FTIR characterization of the organic extraction solutions

The FTIR spectrum of pristine T2EHDGA in n-dodecane (referenced against n-dodecane) is shown in Figure 5A along with the assignment of the observed vibrations. The vibrational bands of the amide functionality on pristine DGA have been assigned as C = O (1660 cm^{-1}) and C–N (1380 and 1426 cm^{-1}, respectively).[33,38–42] In addition to the carbonyl stretch, the ether C–O–C stretch at 1118 cm^{-1} can be used as a marker to monitor changes of T2EHDGA speciation upon equilibration with the aqueous solutions.[33,43] Although contact with water does not change any spectral features of T2EHDGA, equilibration with HNO_3 resulted in significant spectral changes. All of the spectra in Figure 5A were referenced against n-dodecane unless otherwise noted.

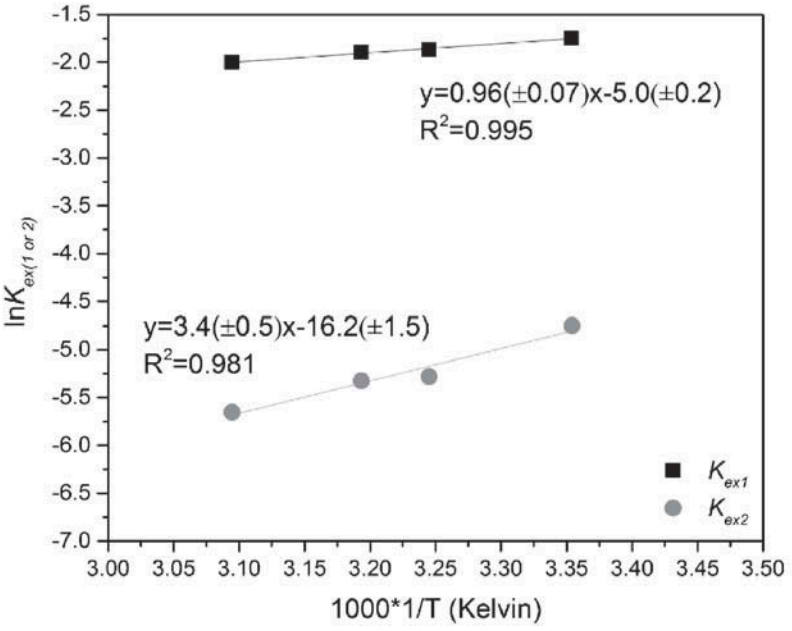

Organic product	ΔH (KJ/mol)	ΔS (J/mol·K)
HNO_3·T2EHDGA	–7.98 ± 0.54	–41.30 ± 1.75
$(HNO_3)_2$·T2EHDGA	–28.16 ± 3.99	–134.4 ± 12.9

Figure 4. Temperature dependence of equilibrium extraction constants (K_{ex1} and K_{ex2}) corresponding to Equations 2 and 3 at 25–50°C. Inset: calculated standard enthalpy and entropy changes.

Upon contact with 1.25 M HNO_3, the absorbance band at 1660 cm^{-1} increases, and a new band grows in at 1604 cm^{-1} as indicated by the red trace in Figure 5A. The free carbonyl and the 1:1 HNO_3·T2EHDGA species both contribute to the absorbance at 1660 cm^{-1}, along with the O–NO_2 asymmetric stretch of the extracted acid, explaining the increase in absorbance at 1660 cm^{-1} as HNO_3 is extracted.[44] The lack of the observable shift of the carbonyl band upon 1:1 HNO_3·T2EHDGA adduct formation was attributed to the overall broadness of this band precluding its differentiation. The speciation diagram (Figure 5E) predicts predominately the 1:1 species at 1.25 M HNO_3, but the contribution of the 2:1 species cannot be discounted as is evident from the in-growth of a new carbonyl peak appearing at 1604 cm^{-1}. When the aqueous HNO_3 concentration is increased to 3 M (blue bold trace), there is a decrease in the 1660 cm^{-1} region and an increase in the intensity of the carbonyl attributed to the 2:1 species. Additionally, the extracted HNO_3 is evident from the O–N–O symmetric stretch at 1292 cm^{-1} and the N–OH symmetric stretch at 945 cm^{-1}, with intensities increasing from 1.25 M to 3 M as the extracted HNO_3 increases.[38]

Equilibration of 0.1 M T2EHDGA with >5 M HNO_3 has a strong tendency for third-phase formation as discussed previously and observed with VPO measurements. Equal volumes of 0.1 M T2EHDGA and 6 M HNO_3 were contacted, and the third phase was isolated and analyzed. The spectrum obtained from the heavy organic phase, represented by the purple trace (dots), was scaled by 0.1 for ease of comparison and was not referenced to *n*-dodecane as a diluent. The third phase is viscous and colorless, and forms where the interface meets the side of the containment. It is evident that the third phase closely resembles the HNO_3-loaded organic phase after contact with 3 M HNO_3, with one exception: the C–O–C stretch, originating at 1118 cm^{-1} in the pristine solvent, shifts to 1166 cm^{-1} in the heavy organic phase. There is some

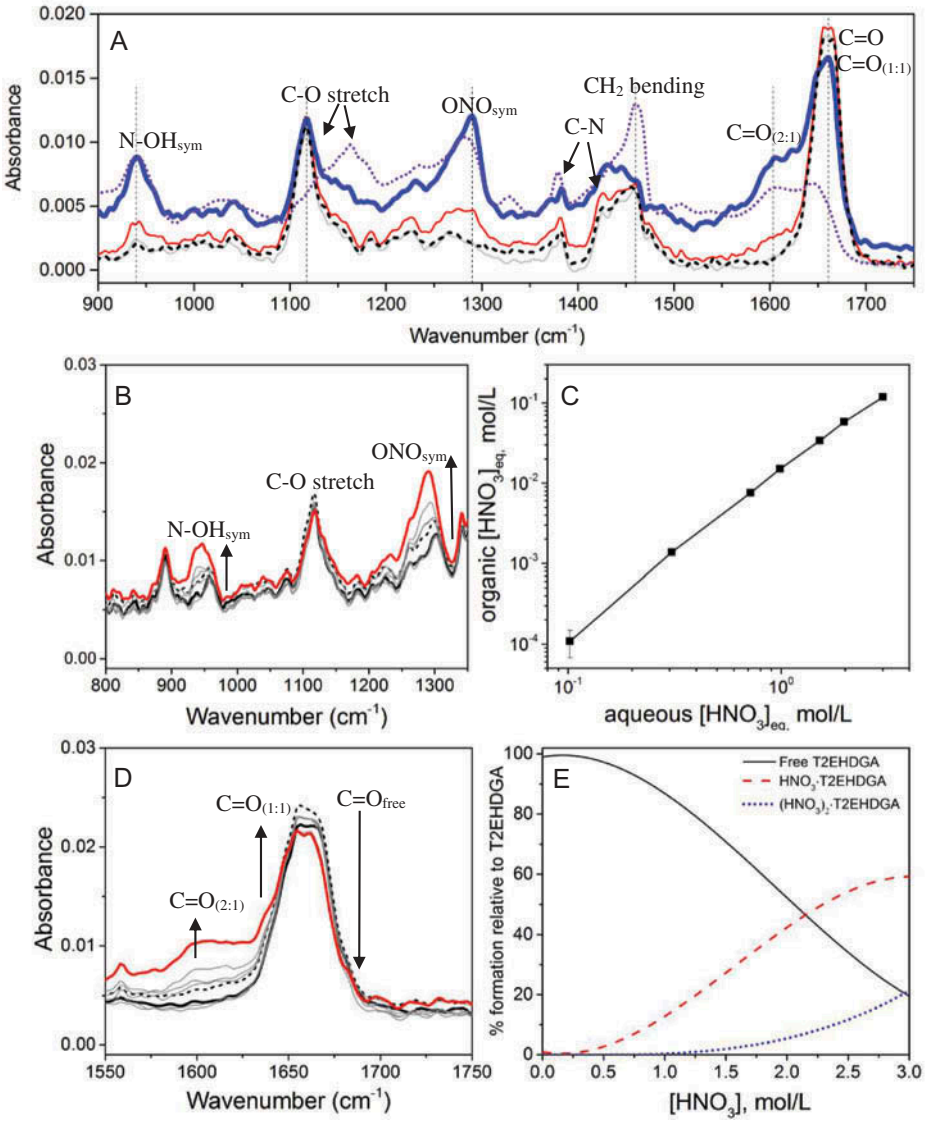

Figure 5. FTIR spectral overlays of 0.1 M T2EHDGA in *n*-dodecane for (A) pristine (light gray), water (dashed), and after contact with 1.25 M (red) and 3 M (blue bold) HNO_3. These spectra were referenced against *n*-dodecane. The heavy organic phase (third phase) obtained from contact with 6 M HNO_3 is shown by the purple trace (dots) and was multiplied by a factor of 0.1 to scale the spectra for visual comparison. This spectrum was not referenced with *n*-dodecane, as the third phase does not contain *n*-dodecane as the diluent. (B, D) Titration of 0.1 M T2EHDGA in *n*-dodecane after contact with aqueous solutions containing HNO_3 from 0.1 (gray) to 3 M (red). The black dashed line is representative of 0.1 M T2EHDGA in *n*-dodecane after contact with aqueous 1 M HNO_3. The solid black line corresponds to 0.1 M T2EHDGA in *n*-dodecane after contact with H_2O. These spectra were referenced to, and the arrows indicate spectral changes as the organic-phase HNO_3 concentration increases. (C) Ion-chromatography results for HNO_3 extracted by 0.1 M T2EHDGA in *n*-dodecane contacted with (0.1–3 M) HNO_3 at 25°C. (E) Speciation diagram of HNO_3·T2EHDGA and $(HNO_3)_2$·T2EHDGA as determined from the SXLSQI modeling results.

indication of this shift in the organic phase after contact with 3 M HNO_3 where a broad peak centered at about 1150 cm^{-1} is observed. This indicates a change in T2EHDGA speciation in the HNO_3-saturated third phase. The shift in the carbonyl region to lower wavenumber is indicative of bound HNO_3 with contribution of both the 1:1 and 2:1 species and is supported by the presence of both the N–OH symmetric stretch and the O–N–O symmetric stretch at 945 and 1292 cm^{-1}, respectively.

The FTIR spectra of 0.1 M T2EHDGA in *n*-dodecane contacted with increasing HNO_3 concentrations from 0.1 to 3 M (referenced to air) are shown in Figure 5B and D. In Figure 5B, there is an increase in the absorbance of the O–N–O symmetric stretch at 1295 cm^{-1}, consistent with an increase in the organic-phase HNO_3 concentration as shown in Figure 5C.[45] As the concentration of HNO_3 in the organic phase increases, the two distinguishable vibrational frequencies near 950 cm^{-1} are no longer discernible with the appearance of the N–OH symmetric stretch (952 cm^{-1}).[46]

Figure 5D highlights the DGA carbonyl vibration centered at about 1660 cm^{-1}. The black trace corresponds to 0.1 M T2EHDGA in *n*-dodecane equilibrated with H_2O. Upon contact with HNO_3 concentrations of 0.1–1 M, there is an increase in the absorbance of the 1660 cm^{-1} carbonyl stretch, with a maximum observed after contact with aqueous 1 M HNO_3 (black dashed line). This is due to the formation of a 1:1 HNO_3·T2EHDGA species speculated as water bridging the carbonyl on T2EHDGA and extracted HNO_3. Again, the contribution of the 1:1 HNO_3·T2EHDGA species, in addition to the O–NO_2 asymmetric stretch of extracted acid, explains the increase in the absorbance at 1660 cm^{-1}.[44,45]

Upon equilibration of 0.1 M T2EHDGA in *n*-dodecane with aqueous HNO_3 concentrations of >1 M (dotted line, Figure 5D), the ingrowth of a new carbonyl peak is observed at 1604 cm^{-1}. According to the speciation diagram in Figure 5E, the $(HNO_3)_2$·T2EHDGA species is observed at aqueous HNO_3 concentrations in excess of 1 M HNO_3. Thus, the appearance of the new carbonyl stretch observed for the 2:1 species is due to a change in speciation of the DGA carbonyl, where HNO_3 is directly hydrogen-bonded to the carbonyl rather than bridged by a water molecule, as observed for the 1:1 species. This observation is in excellent agreement with the results from Karl Fischer titrations, where a significant increase in water extraction is observed at aqueous HNO_3 concentrations > 1 M HNO_3 (Figure 1B), where the $(HNO_3)_2$·T2EHDGA species is responsible for the co-extraction of H_2O. The appearance of a shoulder on the 1660 cm^{-1} carbonyl stretch as the organic HNO_3 concentration increases can be attributed to the O–NO_2 asymmetric stretch of the extracted acid.[45]

NMR spectroscopy

NMR spectroscopy using ^{13}C, ^{1}H, and ^{15}N nuclei was used to further probe the H_2O/HNO_3/T2EHDGA/*n*-dodecane system. When analyzing ^{13}C NMR and ^{1}H NMR measurements, the spectral regions of T2EHDGA overlapping with those of *n*-dodecane were excluded from consideration.

Figure 6 shows the ^{13}C NMR spectrum of the pristine 0.1 M T2EHDGA solution in *n*-dodecane and identifies the considered carbon resonances. The carbon resonances for carbons 3 and 4 do not appear chemically equivalent, although T2EHDGA is a symmetric molecule. The restricted rotation about the C–N bond (on the order of 20 kcal/mol), which is slower than the NMR time scale at room temperature, results in distinct resonances at 50.0 and 47.4 ppm.[47] In agreement with the FTIR observations, the ^{13}C resonances due to the T2EHDGA carbonyl and ether groups (noted as carbons 1 and 2 in Figure 6) are identical in the pristine and water-saturated systems appearing at 168.4 and 70.0 ppm, respectively, indicative of only weak hydrogen bonding with water. This behavior was explained above by a replacement of the T2EHDGA molecule in the van der Waals dimeric species with hydrogen bonding to water, which may not be a significant enough perturbation to result in a detectable carbonyl shift.

Upon contact with HNO_3, the T2EHDGA carbonyl shifts downfield linearly with organic-phase HNO_3 concentration (Figure 6A, inset), which can be attributed to a hydrogen bond interaction between the carbonyl oxygen and the proton from HNO_3. The resonance of carbon 2, however, shifts upfield, in the opposite direction of the carbonyl carbon. This is consistent with the γ-effect, where the carbon beta and the carbon gamma to a substitution frequently shift in opposite directions of one another.[48] Carbons bonded to the amide nitrogen (labeled 3 and 4) shift downfield as the organic acid concentration increases. T2EHDGA carbonyl resonance undergoes only slight

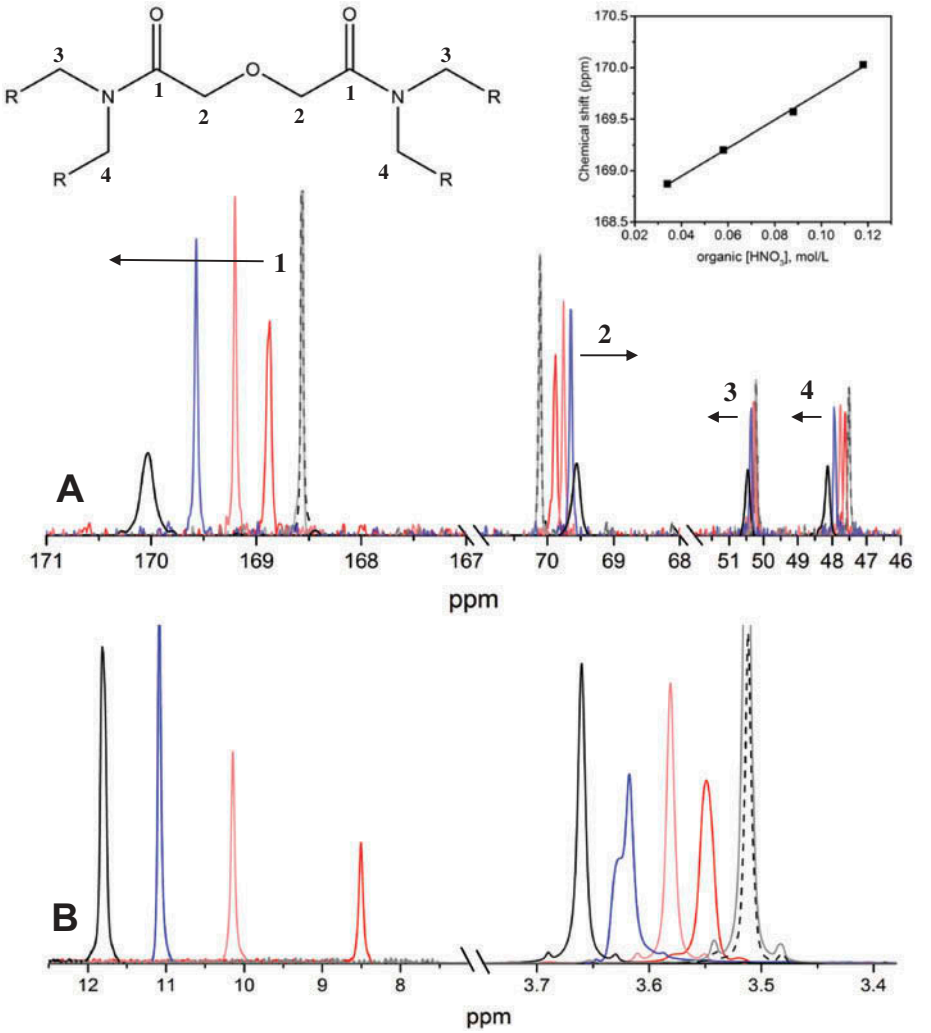

Figure 6. (A) ^{13}C NMR and (B) ^{1}H NMR spectral overlays of pristine 0.1 M T2EHDGA in *n*-dodecane (gray) or after contact with water (black dash), and variable concentrations of HNO_3 1.5 M (red), 2 M (pink), 2.5 M (blue), and 3 M (black). Arrows indicate spectral changes as the organic HNO_3 concentration increases.

broadening in organic solutions contacted with aqueous HNO_3 solution up to 2.5 M, which was attributed to the dominant occurrence of the HNO_3·T2EHDGA species. The carbonyl resonance corresponding to the 0.1 M T2EHDGA solution in *n*-dodecane equilibrated with 3 M HNO_3 exhibited significant broadening. Similar increase in broadening was observed for the ether and nitrogen-bonded alkyl carbon resonances. These findings are in agreement with the FTIR and VPO results and suggest significant change in the organic T2EHDGA speciation, presumably due to the formation of $(HNO_3)_2$·T2EHDGA and possibly higher-order aggregates.

The ^{1}H NMR spectrum of the pristine 0.1 M T2EHDGA/*n*-dodecane contains only one singlet resonance, due to protons bonded to carbon 2, that is free from overlapping *n*-dodecane resonances. It appears at 3.55 ppm and does not change in the water-saturated system. The 0.1 M T2EHDGA/*n*-dodecane equilibrated with aqueous solutions of variable concentrations of HNO_3 shows the appearance of a resonance due to an acidic proton, which steadily shifts downfield as the organic HNO_3 concentration increases (Figure 6B). This shift was attributed to the combination of fast exchange between HNO_3 and water protons as well as due to the change in HNO_3 speciation due to successive binding to T2EHDGA and

the gradual increase of the concentration of $(HNO_3)_2$·T2EHDGA at the expense of the HNO_3·T2EHDGA species. The protons attached to carbon 2 also gradually shift downfield with the addition of HNO_3 as shown in Figure 6, albeit to a lesser extent than the acidic proton shift.

Samples of 0.1 M T2EHDGA in *n*-dodecane were contacted with variable concentrations of ^{15}N-labeled HNO_3 (98+% ^{15}N) to investigate its extraction speciation. One advantage of ^{15}N NMR is that the nitrogen-15 nucleus is spin one half, which results in narrow line widths, but the low gyromagnetic ratio and 0.37% natural abundance result in low sensitivity, which in turn requires long acquisition times. Nevertheless, a single resonance at –265.23 ppm due to the naturally abundant ^{15}N in the amide group was observed for T2EHDGA in *n*-dodecane prior to contact with HNO_3 (Figure 7). Upon contact with $H^{15}NO_3$, a second resonance appears downfield at around –35 ppm, with a corresponding downfield shift of the naturally abundant ^{15}N in T2EHDGA. As the organic HNO_3 concentration increases, both the ^{15}N resonances due to HNO_3 and T2EHDGA continue to shift downfield. This is indicative of a change in the coordination environment about the nitrogen in the extracted HNO_3 as HNO_3 in the organic phase increases, suggesting continual change in speciation upon HNO_3 extraction. The predominant species at 0.5 M HNO_3 is the 1:1 HNO_3·T2EHDGA species, and the gradual increase in the abundance of the $(HNO_3)_2$·T2EHDGA species accounts for the shift at 2 M HNO_3. Upon contact with aqueous 5 M $H^{15}NO_3$, the farthest downfield shifts are observed for both the naturally abundant ^{15}N-T2EHDGA resonance and the resonance associated with extracted HNO_3, which can be attributed to acid-driven aggregation of the organic phase, in agreement with VPO studies.

Conclusions

This work demonstrates that the extraction of HNO_3 by T2EHDGA in *n*-dodecane can be adequately described by the formation of two organic species, HNO_3·T2EHDGA and $(HNO_3)_2$·T2EHDGA. Characterization using FTIR, ^{13}C, ^{1}H, and ^{15}N NMR spectroscopies provides strong evidence of the interaction of HNO_3 through the T2EHDGA carbonyl along with the successive binding of HNO_3 in

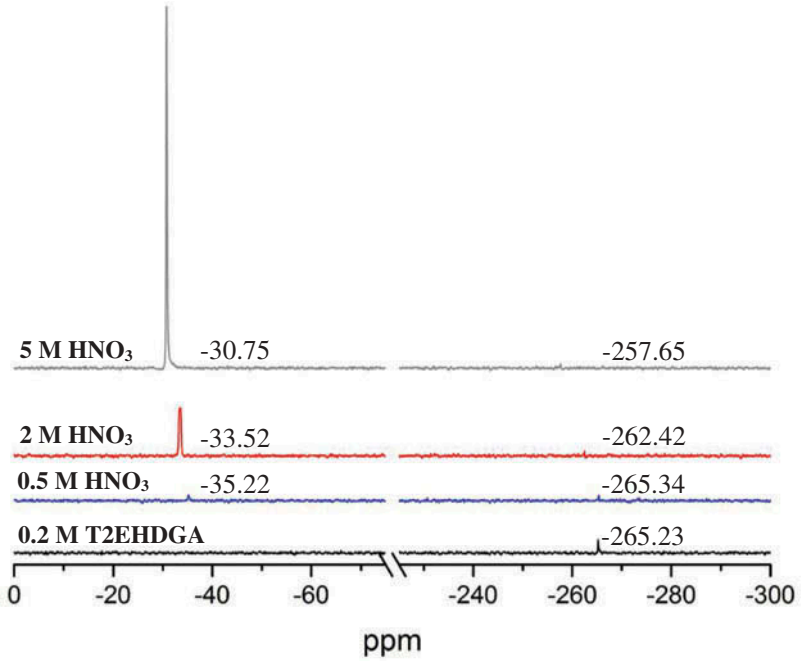

Figure 7. ^{15}N NMR spectral overlay and chemical shifts of pristine 0.2 M T2EHDGA in *n*-dodecane (black) and 0.1 M T2EHDGA/*n*-dodecane after contact with 0.5 M HNO_3 (blue), 2 M HNO_3 (red), and 5 M HNO_3 (gray).

support of the formation of 1:1 species and 2:1 HNO_3·T2EHDGA and $(HNO_3)_2$·T2EHDGA in the organic solutions equilibrated with aqueous < 3 M HNO_3 solutions. As the aqueous acidity approaches 3 M HNO_3, there is evidence of aggregation behavior in the organic phase as indicated by VPO, which eventually leads to third-phase formation. This aggregation behavior has been found to be dependent on both extractant concentration and aqueous acidity. It was found that HNO_3 co-extracts a significant amount water into the organic phase. Variable-temperature studies on the extraction of HNO_3 indicate that the reactions are exothermic, with a slightly greater temperature dependence for the higher-order HNO_3 species.

Funding

This work was supported by U.S. Department of Energy, Office of Nuclear Energy, through the Fuel Cycle Research and Development Program. Pacific Northwest National Laboratory is operated by Battelle Memorial Institute for the U.S. Department of Energy under contract DE-AC05-76RL01830.

ORCID

Gregg J Lumetta http://orcid.org/0000-0002-0216-8515

References

[1] Chu, S.; Majumdar, A. Opportunities and Challenges for a Sustainable Energy Future. *Nature*. 2012, 488(7411), 294–303. doi:10.1038/nature11475.
[2] Macfarlane, A.; Miller, M. Nuclear Energy and Uranium Resources. *Element*. 2007, 3(3), 185–192. doi:10.2113/gselements.3.3.185.
[3] Wigeland, R. A.; Bauer, T. H.; Fanning, T. H.; Morris, E. E. Spent Nuclear Fuel Separations and Transmutation Criteria for Benefit to a Geologic Repository. *Proc. of Waste Management '04*, Tucson, AZ 2004.
[4] Tachimori, S.; Morita, Y. Overview of Solvent Extraction Chemistry for Reprocessing. *Ion Exchange and Solvent Extraction*; Moyer B. Ed.; CRC Press: Boca Raton, 2010, pp. 1–63.
[5] Bell, K.; Geist, A.; McLachlan, F.; Modolo, G.; Taylor, R.; Wilden, A. Nitric Acid Extraction into TODGA. *Procedia Chem.* 2012, 7, 152–159. doi:10.1016/j.proche.2012.10.026.
[6] IAEA. Implication of Partioning and Transmutation in Radioactive Waste Management. *Tech. Reports Ser.* 2004, 435, STI/DOC/010/435.
[7] Rydberg, J.; Cox, M.; Musikas, C.; Choppin, G. R. *Solvent Extraction Principles and Practice*, 2nd; Marcel Dekker: New York, 2004.
[8] Clark, D. L.; The Chemical Complexities of Plutonium. *Los. Alamos Sci.* 2000, 26, 364–381.
[9] Magnusson, D.; Christiansen, B.; Foreman, M. R. S.; Geist, A.; Glatz, J.-P.; Malmbeck, R.; Modolo, G.; Serrano-Purroy, D.; Sorel, C. Demonstration of a SANEX Process in Centrifugal Contactors Using the CyMe4-BTBP Molecule on a Genuine Fuel Solution. *Solvent Extr Ion Exch.* 2009, 27(2), 97–106. doi:10.1080/07366290802672204.
[10] Nash, K. L.; The Chemistry of TALSPEAK: A Review of the Science. *Solvent Extr. Ion Exch.* 2015, 33(1), 1–55. doi:10.1080/07366299.2014.985912.
[11] Nash, K. L. A.; Review of the Basic Chemistry and Recent Developments in Trivalent f-Elements Separations. *Solvent Extr. Ion Exch.* 1993, 11(4), 729–768. doi:10.1080/07366299308918184.
[12] Yaita, T.; Herlinger, A. W.; Thiyagarajan, P.; Jensen, M. P. Influence of Extractant Aggregation on the Extraction of Trivalent f-Element Cations by a Tetraalkyldiglycolamide. *Solvent Extr Ion Exch.* 2004, 22(4), 553–571. doi:10.1081/SEI-120039640.
[13] Gujar, R. B.; Ansari, S. A.; Mohapatra, P. K.; Manchanda, V. K. Development of T2EHDGA Based Process for Actinide Partitioning. Part I: Batch Studies for Process Optimization. *Solvent Extr Ion Exch.* 2010, 28(3), 350–366. doi:10.1080/07366291003685383.
[14] Ansari, S. A.; Pathak, P.; Mohapatra, P. K.; Manchanda, V. K. Chemistry of Diglycolamides: Promising Extractants for Actinide Partitioning. *Chem. Rev.* 2012, 112(3), 1751–1772. doi:10.1021/cr200002f.
[15] Modolo, G.; Asp, H.; Vijgen, H.; Malmbeck, R.; Magnusson, D.; Sorel, C. Demonstration of a TODGA-Based Continuous Counter-Current Extraction Process for the Partitioning of Actinides from a Simulated PUREX Raffinate, Part II: Centrifugal Contactor Runs. *Solvent Extr. Ion Exch.* 2008, 26(1), 62–76. doi:10.1080/07366290701784175.

[16] Madic, C.; Boullis, B.; Baron, P.; Testard, F.; Hudson, M. J.; Liljenzin, J. O.; Christiansen, B.; Ferrando, M.; Facchini, A.; Geist, A.; Modolo, G.; Espartero, A. G.; De Mendoza, J. Futuristic Back-End of the Nuclear Fuel Cycle with the Partitioning of Minor Actinides. *J. Alloys Compd.* 2007, 444–445(SPEC. ISS.), 23–27. doi:10.1016/j.jallcom.2007.05.051.

[17] Gelis, A. V.; Lumetta, G. J. Actinide Lanthanide Separation Process – ALSEP. *Ind. Eng. Chem. Res.* 2014, 53(4), 1624–1631. doi:10.1021/ie403569e.

[18] Lumetta, G. J.; Gelis, A. V.; Carter, J. C.; Niver, C. M.; Smoot, M. R. The Actinide-Lanthanide Separation Concept. *Solvent Extr Ion Exch.* 2014, 32(4), 333–347. doi:10.1080/07366299.2014.895638.

[19] Ansari, S. A.; Mohapatra, P. K.; Prabhu, D. R.; Manchanda, V. K. Transport of Americium(III) through a Supported Liquid Membrane Containing N,N,N',N'-tetraoctyl-3-Oxapentane Diamide (TODGA) in N-Dodecane as the Carrier. *J. Memb. Sci.* 2006, 282(1–2), 133–141. doi:10.1016/j.memsci.2006.05.013.

[20] Baes, C. F.; *SXLSQI, Jr. A Program for Modeling Solvent Extraction Systems*; Report ORNL/TM-13604; Oak Ridge National Laboratory: Oak Ridge Tennessee, 1998.

[21] Levitskaia, T. G.; Bryan, J. C.; Sachleben, R. A.; Lamb, J. D.; Moyer, B. A. A Surprising Host-Guest Relationship between 1,2-Dichloroethane and the Cesium Complex of Tetrabenzo-24-Crown-8. *J. Am. Chem. Soc.* 2000, 122 (4), 554–562. doi:10.1021/ja992760j.

[22] Baes, C. F. J.; Moyer, B. A.; Case, G. N.; Case, F. I. SXLSQI: A Computer Program for Including Both Complex Formation and Activity Effects in the Interpretation of Solvent Extraction Data. *Sep. Sci. Technol.* 1990, 25(13–15), 1675–1688. doi:10.1080/01496399008050416.

[23] Millero, F. J.; *Water and Aqueous Solutions*, Horne R. A. Ed.; Wiley-Interscience: New York, 1971.

[24] Barton, A. F. M.; *CRC Handbook of Solubility Parameters and Other Cohesion Parameters*; CRC Press: Boca Raton, 1991.

[25] Herbst, R. S.; Peterman, D. R.; Zalupski, P. R.; Nash, K. L.; Tillotson, R. D.; Delmau, L. H. Thermodynamics of Cesium Extraction from Acidic Media by HCCD and PEG. *Solvent Extr Ion Exch.* 2010, 28(5), 563–578. doi:10.1080/07366299.2010.502865.

[26] Pitzer, K. *Activity Coefficients in Electrolyte Solutions*, 2nd; Pitzer K. S. Ed.; CRC Press: Boca Raton, 1991.

[27] Nichols, T. T.; Taylor, D. D. *Thermodynamic Phase and Chemical Equilibrium at 0-110° C for the H^+-K^+-Na^+-Cl–H_2O System up to 16 Molal and the HNO_3-H_2O System up to 20 Molal Using an Association-Based Pitzer Model Compatible with ASPEN Plus*, Report INEEL/EXT-03-01167, Idaho National Engineering and Environmental Laboratory, Idaho Falls, Idaho, USA, 2003.

[28] Gottlieb, H. E.; Kotlyar, V.; Nudelman, A. NMR Chemical Shifts of Common Laboratory Solvents as Trace Impurities. *J. Org. Chem.* 1997, 62(3), 7512–7515. doi:10.1021/jo971176v.

[29] Evans, W. J.; Rego, D. B.; Ziller, J. W. Synthesis, Structure, and ^{15}N NMR Studies of Paramagnetic Lanthanide Complexes Obtained by Reduction of Dinitrogen. *Inorg Chem.* 2006, 45(26), 10790–10798. doi:10.1021/ic061485g.

[30] Jensen, M. P.; Yaita, T.; Chiarizia, R. Reverse-Micelle Formation in the Partitioning of Trivalent F-Element Cations by Biphasic Systems Containing a Tetraalkyldiglycolamide. *Langmuir.* 2007, 23(9), 4765–4774. doi:10.1021/la0631926.

[31] Deepika, P.; Sabharwal, K. N.; Srinivasan, T. G.; Vasudeva Rao, P. R. Studies on the Use of N,N,N′,N′-Tetra(2-Ethylhexyl) Diglycolamide (TEHDGA) for Actinide Partitioning II: Investigation on Radiolytic Stability. *Solvent Extr Ion Exch.* 2011, 29(2), 230–246. doi:10.1080/07366299.2011.539145.

[32] Nave, S.; Modolo, G.; Madic, C.; Testard, F. Aggregation Properties of *N, N, N′, N′*-Tetraoctyl-3-oxapentane-diamide (TODGA) in *N*-Dodecane. *Solvent Extr Ion Exch.* 2004, 22(4), 527–551. doi:10.1081/SEI-120039721.

[33] Sasaki, Y.; Rapold, P.; Arisaka, M.; Hirata, M.; Kimura, T.; Hill, C.; Cote, G. An Additional Insight into the Correlation between the Distribution Ratios and the Aqueous Acidity of the TODGA System. *Solvent Extr. Ion Exch.* 2007, 25(2), 187–204. doi:10.1080/07366290601169345.

[34] Ravi, J.; Suneesh, A. S.; Prathibha, T.; Venkatesan, K. A.; Antony, M. P.; Srinivasan, T. G.; Vasudeva Rao, P. R. Extraction Behavior of Some Actinides and Fission Products from Nitric Acid Medium by a New Unsymmetrical Diglycolamide. *Solvent Extr Ion Exch.* 2011, 29(1), 86–105. doi:10.1080/07366299.2011.539421.

[35] Pathak, P. N.; Ansari, S. A.; Mohapatra, P. K.; Manchanda, V. K.; Patra, A. K.; Aswal, V. K. Role of Alkyl Chain Branching on Aggregation Behavior of Two Symmetrical Diglycolamides: Small Angle Neutron Scattering Studies. *J. Colloid Interface Sci.* 2013, 393(1), 347–351. doi:10.1016/j.jcis.2012.10.023.

[36] Gujar, R. B.; Ansari, S. A.; Murali, M. S.; Mohapatra, P. K.; Manchanda, V. K. Comparative Evaluation of Two Substituted Diglycolamide Extractants for "Actinide Partitioning". *J. Radioanal. Nucl. Chem.* 2010, 284(2), 377–385. doi:10.1007/s10967-010-0467-y.

[37] Arisaka, M.; Kimura, T. Thermodynamic and Spectroscopic Studies on Am(III) and Eu(III) in the Extraction System of *N, N, N ', N '*-Tetraoctyl-3-Oxapentane-1,5-Diamide in *N* -Dodecane/Nitric Acid. *Solvent Extr Ion Exch.* 2011, 29(1), 72–85. doi:10.1080/07366299.2011.539127.

[38] Ravi, J.; Venkatesan, K. A.; Antony, M. P.; Srinivasan, T. G.; Vasudeva Rao, P. R. Tuning the Diglycolamides for Modifier-Free Minor Actinide Partitioning. *J. Radioanal. Nucl. Chem.* 2013, 295(2), 1283–1292. doi:10.1007/s10967-012-1905-9.

[39] Reilly, S. D.; Gaunt, A. J.; Scott, B. L.; Modolo, G.; Iqbal, M.; Verboom, W.; Sarsfield, M. J. Plutonium(Iv) Complexation by Diglycolamide Ligands—Coordination Chemistry Insight into TODGA-Based Actinide Separations. *Chem. Commun.* 2012, 48(78), 9732. doi:10.1039/c2cc34967a.

[40] Mowafy, E. A.; Mohamed, D. Extraction of Rare Earth Elements from Nitrate Solution Using Novel Unsymmetrical Diglycolamide. *Sep. Sci. Technol.* 2017, 52(6), 1006–1014. doi:10.1080/01496395.2016.1274760.

[41] Mowafy, E. A.; Aly, H. F. Extraction Behaviours of Nd(III), Eu(III), La(III), Am(III), and U(VI) with Some Substituted Malonamides from Nitrate Medium. *Solvent Extr Ion Exch*. 2002, 20(2), 177–194. doi:10.1081/SEI-120003020.

[42] Mowafy, E. A.; Mohamed, D. Extraction and Separation of Nd(III), Sm(III), Dy(III), Fe(III), Ni(II), and Cs(I) from Concentrated Chloride Solutions with *N, N, N'*, *N'*-Tetra(2-Ethylhexyl) Diglycolamide as New Extractant. *J Rare Earths*. 2015, 33(4), 432–438. doi:10.1016/S1002-0721(14)60437-3.

[43] Mowafy, E. A.; Mohamed, D. Extraction Behavior of Trivalent Lanthanides from Nitric Acid Medium by Selected Structurally Related Diglycolamides as Novel Extractants. *Sep. Purif. Technol.* 2014, 128, 18–24. doi:10.1016/j.seppur.2014.03.005.

[44] Chiarizia, R.; Jensen, M. P.; Borkowski, M.; Ferraro, J. R.; Thiyagarajan, P.; Littrell, K. C. Third Phase Formation Revisited: The U(VI), HNO_3-TBP, n-Dodecane System. *Solvent Extr Ion Exch*. 2003, 21(1), 1–27. doi:10.1081/SEI-120017545.

[45] Pretsch, E.; Buhlmann, P.; Badertscher, M. *Stucture Determination of Organic Compounds*, 4th; Springer: Heidelberg, 2009.

[46] Levitskaia, T. G.; Peterson, J. M.; Campbell, E. L.; Casella, A. J.; Peterman, D. R.; Bryan, S. A. Fourier Transform Infrared Spectroscopy and Multivariate Analysis for Online Monitoring of Dibutyl Phosphate Degradation Product in Tributyl Phosphate/N -Dodecane/Nitric Acid Solvent. *Ind. Eng. Chem. Res.* 2013, 52(49), 17607–17617. doi:10.1021/ie402722n.

[47] Zabicky, J.; *The Chemistry of Amides*; Interscience Publishers: London, 1970.

[48] Kleinpeter, E.; Seidl, P. R. The Γ-And the Δ-Effects in ^{13}C NMR Spectroscopy in Terms of Nuclear Chemical Shielding (NCS) Analysis. *J. Phys. Org. Chem*. 2004, 17(8), 680–685. doi:10.1002/poc.746.